ELSEVIER

International Journal of Heat and Fluid Flow 19 (1998) 223–232

International Journal of HEAT AND FLUID FLOW

Numerical and experimental study of flow and heat transfer around a tube in cross-flow at low Reynolds number

E. Buyruk [a], M.W. Johnson [b], I. Owen [b,*]

[a] *Department of Mechanical Engineering, The University of Cumhuriyet, 58140 Sivas, Turkey*
[b] *Department of Mechanical Engineering, The University of Liverpool, P.O. Box 147, Liverpool L69 3BX, UK*

Received 16 November 1996; accepted 20 October 1997

Abstract

A numerical and experimental study of the laminar flow and heat transfer characteristics of a cylinder in cross-flow is presented. The computational technique used is a stream function-vorticity formulation of the laminar flow steady state incompressible Navier–Stokes and energy equations and uses a Gauss–Seidel over-relaxation technique to obtain stream function and temperature distributions. Calculations are presented for an isothermally heated single tube in a duct with different blockage ratios. The variation of local Nusselt number, pressure and also isotherm and streamline contours are predicted with Reynolds number of 120 and 390. For the Reynolds number of 390, the local Nusselt number distributions are shown to be similar to those obtained through measurement of the local heat flux from the surface of a tube using a micro-foil heat flow sensor.

Keywords: Convection heat transfer; Cylinders; Heat exchangers; Cross-flow

Notation

B	blockage ratio
D	tube diameter
g	acceleration due to gravity
h_θ	local heat transfer coefficient
k	thermal conductivity
P	pressure
P_θ	local surface static pressure
T	temperature
T_s	surface temperature
T_∞	free stream temperature
V	upstream velocity
W	width of the duct
u, v	velocity components in x and y directions respectively
x, y	cartesian coordinates
$\xi,\ \eta$	orthogonal coordinates
α	thermal diffusivity
ν	kinematic viscosity
ρ	density
ψ	stream function
Ω	vorticity

Non-dimensional numbers

Gr	Grashof number
Re	Reynolds number
Nu	Nusselt number

1. Introduction

Heat exchangers with tube banks in cross-flow are of great practical interest in many thermal and chemical engineering processes. In order to examine the process of flow and heat transfer for a single tube and a tube in a bank and their response to changes of geometry or flow conditions, it is possible to undertake experimental and numerical studies on simple geometrical models. Local surface values and overall flow and temperature distributions can be used to determine the effect of each geometrical or flow parameter. Consequently a large number of experimental and numerical studies have already been carried out to determine heat transfer and flow structures for single tubes and tube banks under different conditions to consider the effects of blockage, of longitudinal or transverse pitch ratios, of Reynolds number and of other conditions. Buyruk et al. (1995) have studied experimentally the local Nusselt number distribution within a single tube row for different blockage ratios in cross-flow for Reynolds numbers between 7960 and 47 770. Akilbayev et al. (reported by Zukauskas, 1972), Perkins and Leppert (1964), West and Apelt (1982) and Hiwada and Mabuchi (1980) have investigated the effect of blockage by either changing duct width or by altering tube diameter in the subcritical Reynolds number range (i.e. laminar boundary layer). Chen et al. (1986), Paolino et al. (1986), and Launder and Massey (1978) have predicted Nusselt number distributions for single tubes in large ducts (i.e. no blockage effects) and for a tube in a bank.

Although it is beneficial to operate heat exchangers in turbulent flow, it is not unusual for them to operate with low

* Corresponding author. E-mail: ieuan@mechnet.liv.ac.uk.

0142-727X/98/$19.00
PII: S0142-727X(97)10027-3

Reynolds number flow. From a review of the literature it is evident that only a few experimental studies have investigated the flow and heat transfer around a tube for low Reynolds numbers. Eckert and Soehngen (1953) used a Mach–Zehnder interferometer to obtain the temperature field in the wake of heated cylinders up to 38.1 mm diameter for low Reynolds numbers. Krall and Eckert (1973) investigated the local heat transfer coefficient around a 4.73 mm cylinder for Reynolds numbers between 7.4 and 4640 without specifying the effect of blockage on the distribution. Dennis et al. (1968) calculated the distribution of heat transfer coefficient around a cylinder in viscous flow with Reynolds number between 0.01 and 40. They were able to show good agreement with experimental data for the average heat transfer coefficient but were unable to make comparisons for the circumferential distribution of heat transfer coefficient due to the absence of experimental data.

For tube banks, the overall flow and heat transfer characteristics have been investigated by several authors. Omohundro et al. (1949) obtained results for the overall pressure drop and heat transfer with laminar flow through a staggered tube bank. Bergelin et al. (1949) undertook similar work for in-line and staggered tube bank geometries. Antonopolous (1985) computed the convection heat transfer in tube assemblies for laminar flow. He calculated both local and average heat transfer coefficients and again the lack of experimental data for the circumferential distribution of heat transfer was evident. Similar observations can be made regarding the study of Faghri and Rao (1987) who computed values for average Nusselt number in finned and unfinned tube banks. More recently

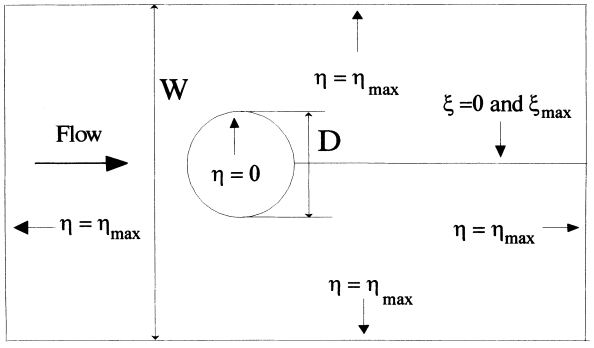

Fig. 1. Confined single cylinder, $B = D/W$.

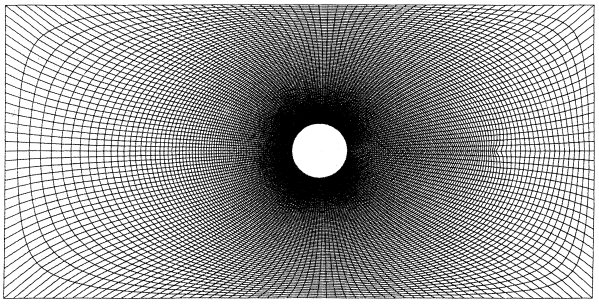

Fig. 2. Computational grid for calculation.

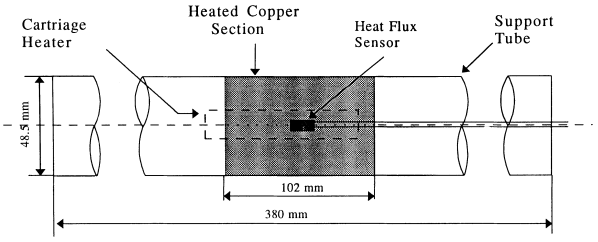

Fig. 3. Instrumented tube.

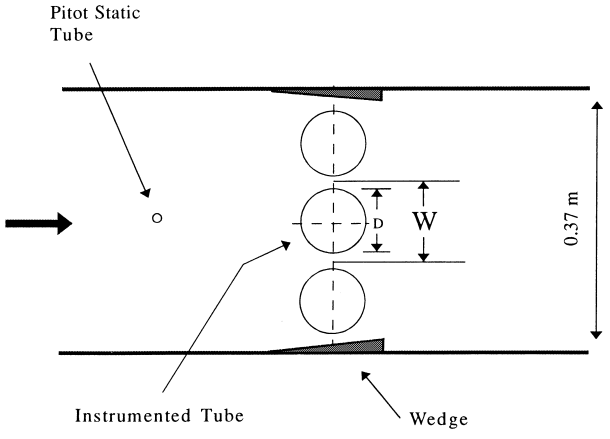

Fig. 4. Wind tunnel.

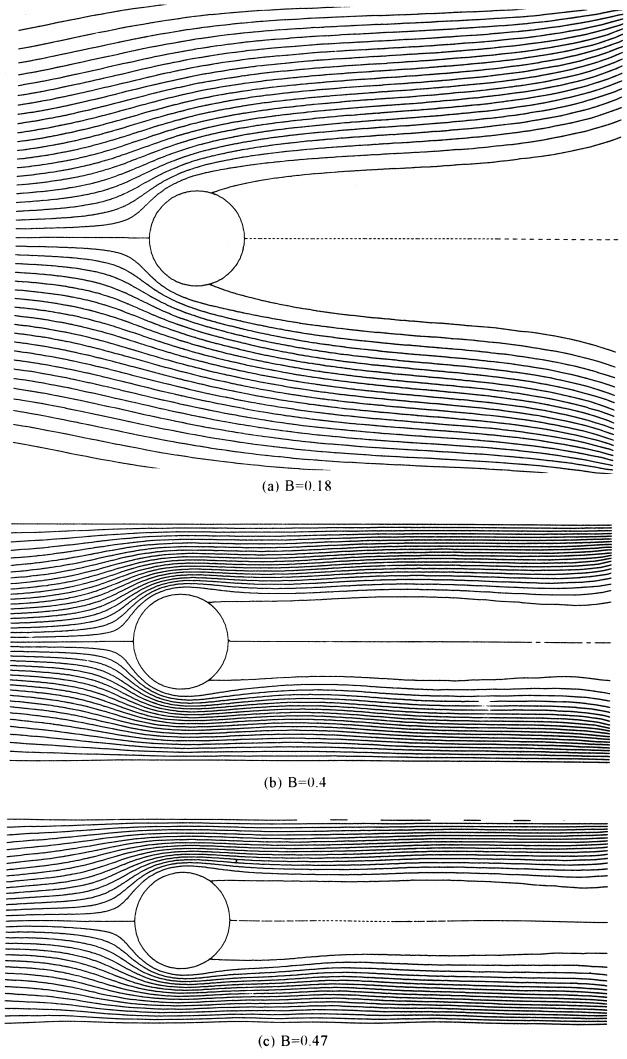

Fig. 5. Streamlines for different blockage ratios with Re = 120.

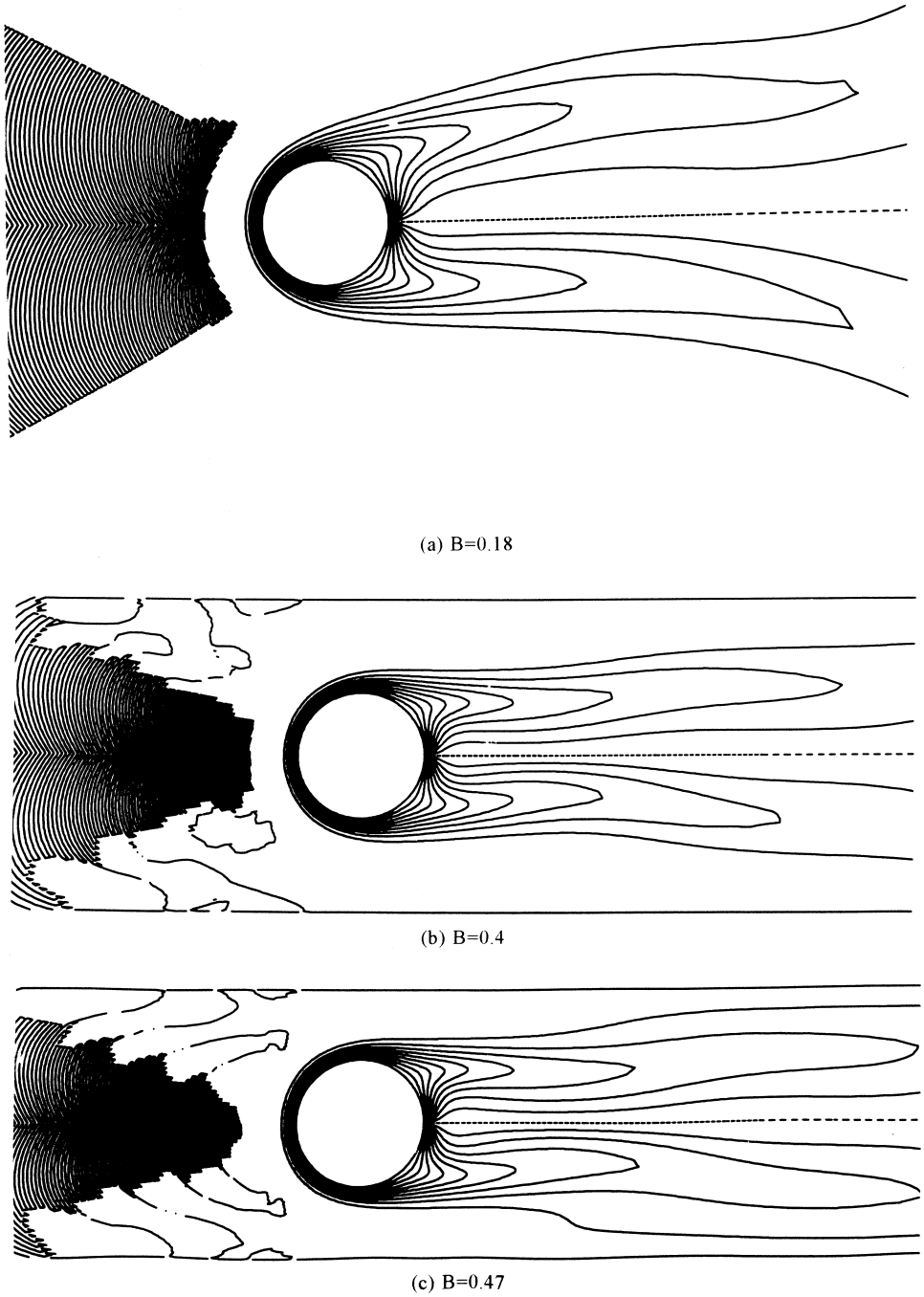

(a) B=0.18

(b) B=0.4

(c) B=0.47

Fig. 6. Isotherms for different blockage ratios with Re = 120.

Zdravistch et al. (1995) carried out a numerical study of both laminar and turbulent heat transfer in tube banks; again, because of the absence of detailed measurements in laminar flow, they had to resort to comparing overall heat transfer coefficients using the data of Bergelin et al. (1949).

There is a relative scarcity of data for heat transfer from tubes and tube banks at low Reynolds numbers and therefore the purpose of this paper is to present results of an investigation into the local variation of heat transfer coefficient around a cylinder in low Reynolds number flow and to consider the effect of varying blockage. The numerical and experimental study considers the effect of blockage on the flow and heat transfer characteristics of a single tube in a duct. The Reynolds numbers used are 120 and 390 and the blockage ratio is varied from 0.18 to 0.47. The computational technique uses the stream function-vorticity formulation to solve the laminar, steady-state Navier–Stokes equations and energy equation. Numerical results are obtained around half the cylinder including the wake zone beyond the separation point. The experimental work involved a heated copper cylinder of 50 mm diameter instrumented with a surface heat flux sensor which was used to obtain the circumferential distribution of heat transfer coefficient. Whilst the experimental data presented is limited in its ranges of Reynolds number and geometry, it nevertheless makes a contribution to this area where data is scarce.

2. Numerical modelling

2.1. Grid

Some flow problems can be solved using an orthogonal co-ordinate system (ξ, η) where ξ and η are known functions of x and y and the flow boundaries are lines of constant ξ or constant η. The grid is then simply made up of lines of constant ξ and constant η. A common example is the cylindrical co-ordinate system. In the present study, the grid generation is based on that of Thompson et al. (1974) as developed by Johnson (1990). The method generates orthogonal curvilinear grids by solving two Laplace equations for ξ and η. In the current work an "O" grid is used where the rectangle $\eta = 0$, η_{max}, $\xi = 0$, ξ_{max} is mapped onto the flow geometry as shown in Fig. 1.

2.2. Computational technique for solving conservation equations

The flow and heat transfer through the geometry is governed by partial differential equations derived from the laws of conservation of mass, momentum and energy. In two dimensions, two momentum and one continuity equation together with the appropriate boundary conditions contain enough information for solution of the velocity components u and v and pressure p at any point. The temperatures can be found by application of the energy equation. In the present study, the computational technique used is a stream function-vorticity formulation of laminar, steady Navier–Stokes equations with assumed constant density, as described by Johnson (1990). Introducing the stream function, ψ, with the continuity equation then

$$\frac{\partial \psi}{\partial y} = u \quad \text{and} \quad -\frac{\partial \psi}{\partial x} = v \tag{1}$$

and the vorticity Ω is then written as

$$\Omega = \frac{\partial u}{\partial y} - \frac{\partial v}{\partial x} = \frac{\partial^2 \psi}{\partial x^2} + \frac{\partial^2 \psi}{\partial y^2} \tag{2}$$

or $\Omega = \nabla^2 \psi$.

Replacing u and v in the momentum equations using Eqs. (1) and (2) then gives:

$$\frac{1}{\rho}\frac{\partial P}{\partial x} + \frac{\partial \psi}{\partial y}\frac{\partial \psi}{\partial x \partial y} - \frac{\partial \psi}{\partial x}\frac{\partial^2 \psi}{\partial y^2} = \nu \frac{\partial \Omega}{\partial y}, \tag{3}$$

$$\frac{1}{\rho}\frac{\partial P}{\partial y} - \frac{\partial \psi}{\partial y}\frac{\partial^2 \psi}{\partial x^2} + \frac{\partial \psi}{\partial x}\frac{\partial \psi}{\partial x \partial y} = -\nu \frac{\partial \Omega}{\partial x}. \tag{4}$$

The solution of these equations is simplified by cross-differentiating with respect to x and y respectively and subtracting to eliminate the pressure terms. This then leads to

$$\nu \nabla^2 \Omega = \frac{\partial \psi}{\partial y}\frac{\partial \Omega}{\partial x} - \frac{\partial \psi}{\partial x}\frac{\partial \Omega}{\partial y}. \tag{5}$$

Eqs. (2) and (5) are solved simultaneously to obtain stream function and vorticity values. Once stream function is known, the velocities can be determined from Eq. (1). The temperature distribution can then be determined from the energy equation as

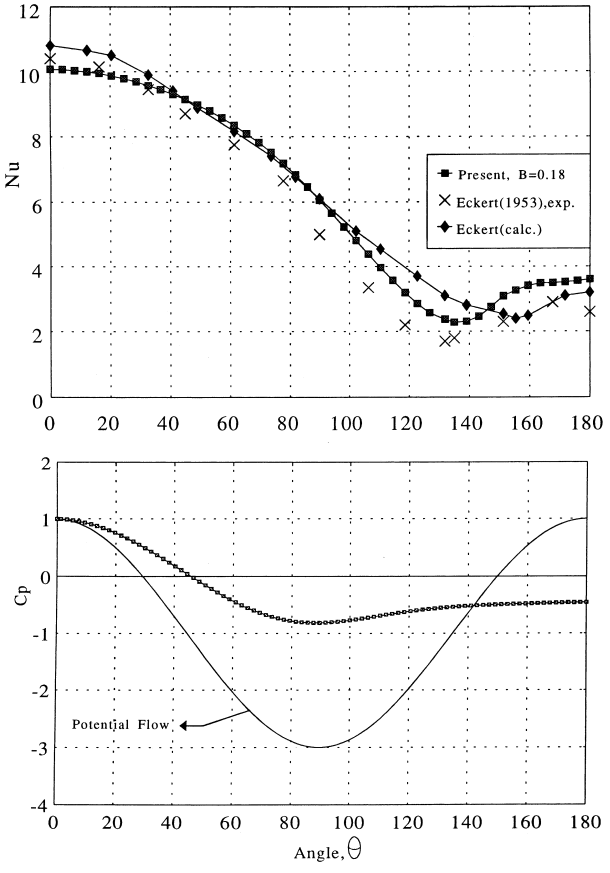

Fig. 7. Calculated local Nusselt number and pressure coefficient for $B = 0.18$ and $\mathrm{Re} = 120$.

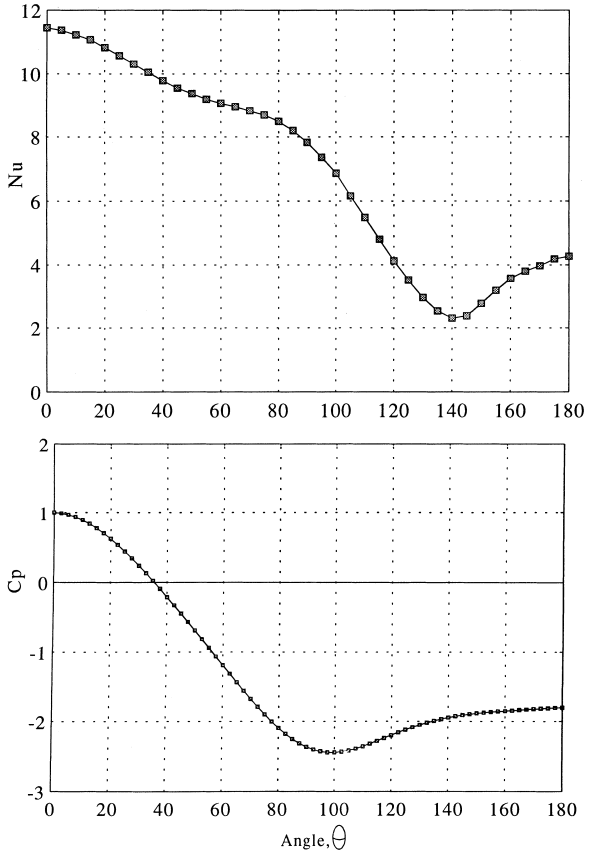

Fig. 8. Calculated local Nusselt number and pressure coefficient for $B = 0.4$ and $\mathrm{Re} = 120$.

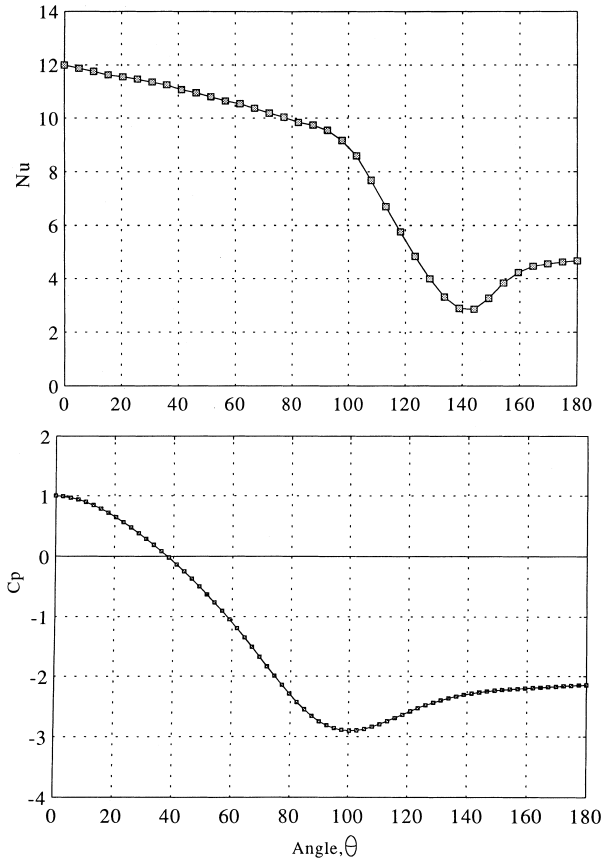

Fig. 9. Calculated local Nusselt number and pressure coefficient for $B = 0.47$ and $\mathrm{Re} = 120$.

$$\frac{\partial T}{\partial x} + v\frac{\partial T}{\partial y} = \alpha\left(\frac{\partial^2 T}{\partial x^2} + \frac{\partial^2 T}{\partial y^2}\right). \tag{6}$$

On the surfaces, u and v are zero and hence the ψ terms in Eqs. (3) and (4) are zero. These equations can therefore be integrated along the surface to obtain the pressure distributions.

The Nusselt number can be obtained since the conductive heat transfer rate of the fluid over the solid boundary equals its convective heat transfer rate

$$-k\left(\frac{\mathrm{d}T}{\mathrm{d}n}\right)_s = h_\theta(T_{\text{surface}} - T_\infty) \tag{7}$$

and the local Nusselt number is given by

$$\mathrm{Nu} = \frac{h_\theta D}{k}. \tag{8}$$

The present scheme utilises second order accuracy centre differencing. Flow and temperature solutions are obtained using a Gauss–Seidel over-relaxation procedure. The numerical solution of the equations was accomplished by transforming the governing Eqs. (2), (5) and (6) onto an orthogonal curvilinear grid. The computer code is described in more detail by Johnson (1990).

2.3. Boundary conditions and computational procedure

The conservation laws governing the flow and heat transfer have been reduced to partial differential equations of stream function, vorticity and temperature. Boundary conditions are used at inlet, outlet, sidewalls and solid-body boundaries. The sidewalls are lines of symmetry between cylinders arranged in a row across the flow.

- In the inlet section, both velocity components are known therefore ψ, and $\partial\psi/\partial n$ can be specified along the inlet boundary, where n is the direction normal to the boundary.
- In the outlet section, assuming the outlet is sufficiently far downstream of the bluff body and the static pressure is constant across the outlet then $\partial\Omega/\partial n = 0$ and $v = 0$ also $\partial\psi/\partial n = 0$.
- On the side boundaries $v = 0$ and so ψ is constant. T is also assumed to be equal to the inlet free stream temperature.
- On the cylinder, again both velocity components are zero and the temperature is constant.

The flow domain under consideration, for a single tube in a row can be seen in Fig. 1. The upper and lower boundaries of the flow domain are lines of symmetry. The blockage ratio is defined as D/W where W is the height between the side walls and D, the diameter of the tube. The blockage ratios used were 0.18, 0.40 and 0.47. The value of 0.18 was selected as being representative of a single tube, a smaller ratio would have been desirable but was computationally expensive. The values 0.40 and 0.47 are typical of heat exchanger geometries.

The computational grid for a blockage ratio of 0.18 is shown in Fig. 2. The O type grid used avoids rapid changes in the spacing of the grid cell near the solid body. The grid is generated in two stages. Firstly the desired point distribution is chosen on the physical domain boundary and secondly the interior coordinate lines are generated to maximise orthogonality with the point distribution on the boundaries. Large variations in the stream function, vorticity and temperature occur near the surface of the body. Therefore, a smaller mesh size close to the surface is desirable with a coarser mesh further from the body. To vary Reynolds number ($\mathrm{Re} = VD/\nu$), the upstream velocity, V, was altered while the tube diameter was kept constant at 0.05656 m and the air viscosity at $1.58 \times 10^{-5}\,\mathrm{m^2/s}$. The stream-function on the boundaries is calculated assuming that the value on the bottom boundary is zero and that the value on the top boundary is $\psi = VW$, where W is the width of the channel.

Predictions were made for the single tube geometry for a range of Reynolds number between 120 and 390. Local Nusselt number was calculated using Eq. (7) and was plotted against the angular position on the tube. The local pressure coefficient was defined as

$$C_\mathrm{p} = 1 + \frac{P_\theta - P_{\theta=0}}{\frac{1}{2}\rho V^2}. \tag{9}$$

Here, V is taken as the upstream velocity and P_θ the surface static pressure at angle θ measured from the front stagnation point.

The Reynolds number used in the calculation is within the range for which buoyancy effects may be safely neglected because the Reynolds number yields a forced convection velocity that is very much higher than the characteristic free convection velocity (Kreith, 1965), thus

$$\frac{\mathrm{Gr}}{\mathrm{Re}^2} < 1, \tag{10}$$

where Gr is the Grashof number

$$\mathrm{Gr} = \frac{g\beta V\,\Delta T\,D^3}{\nu^2}. \tag{11}$$

In the present study $0.036 < \mathrm{Gr}/\mathrm{Re}^2 < 0.558$.

3. Experimental procedure

Experiments were carried out using a thick-walled copper cylinder which was heated internally by an electric cartridge heater and held between two PVC tubes to form a single tube

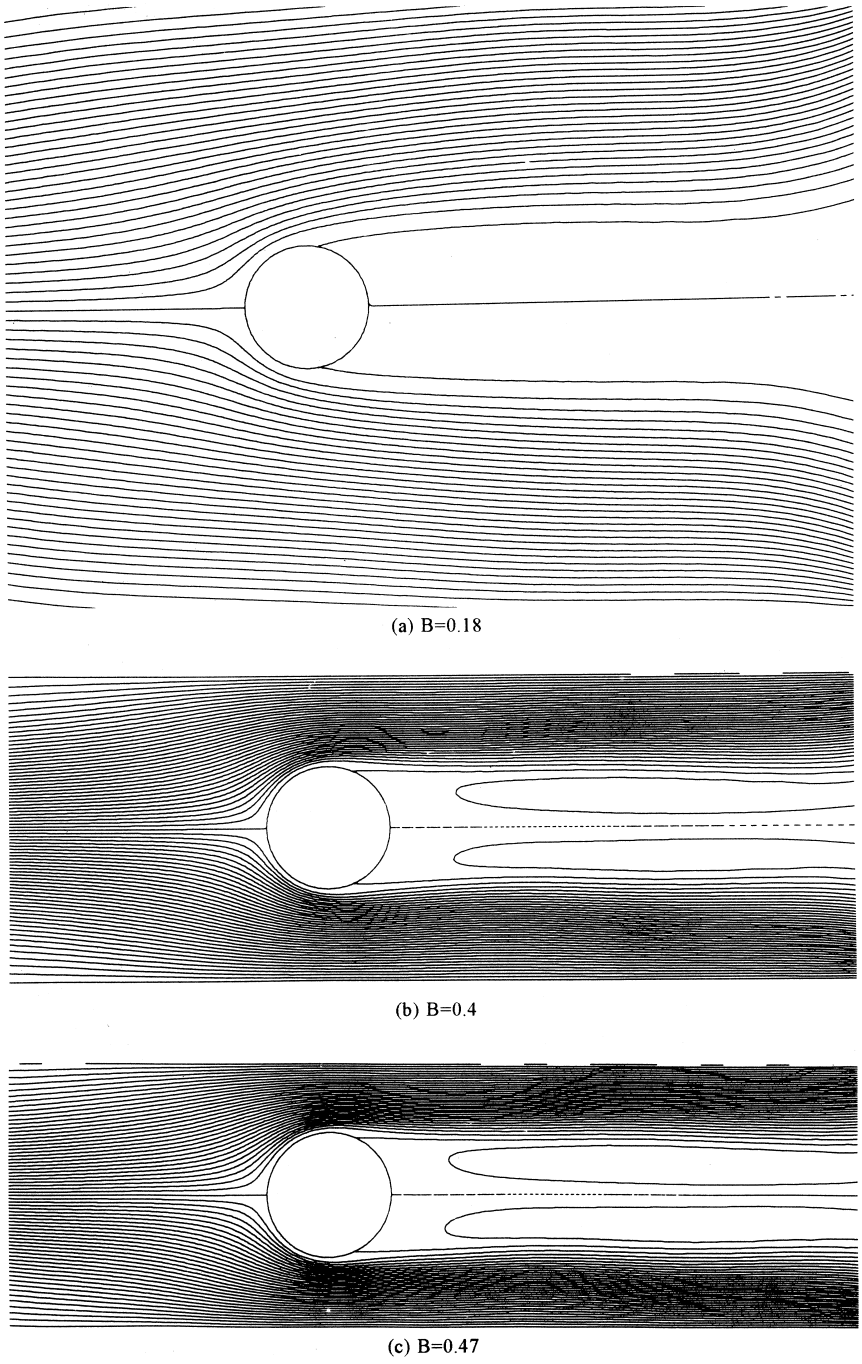

Fig. 10. Streamlines for different blockage ratios with $Re = 390$.

assembly as shown in Fig. 3. The heat flux from the surface of the cylinder was measured using an RdF^{TM} micro-foil heat flux sensor type 27034 attached to the surface with an epoxy resin adhesive. The voltage output from the sensor was connected to a digital multimeter and this reading was converted to heat flux using the calibration factor provided by the sensor manufacturer. Surface temperature was also measured by the heat flux sensor and was recorded by a digital thermometer. It was observed during the experiments that the distribution of surface temperature rarely varied by more than 1°C because of the high thermal conductivity of the copper. In the numerical calculations, therefore, a constant surface temperature was assumed.

Only one heat flux sensor was used on the tube surface and the angular position of the tube was varied from 0° to 360° in 10° steps. A protractor was fitted to one end of the tube to allow the angular location to be monitored. Air temperature was recorded by a mercury thermometer placed into the upstream section.

A row of horizontal tubes was placed in the working section of the wind tunnel as shown in Fig. 4. The spacing of the tubes could be adjusted and slender wedges were used at the end of the row to ensure the correct gap was maintained. Experimentation started with the single instrumented cylinder over a Reynolds number range of 120–390. The heat transfer characteristics obtained were used as the bench-marks against

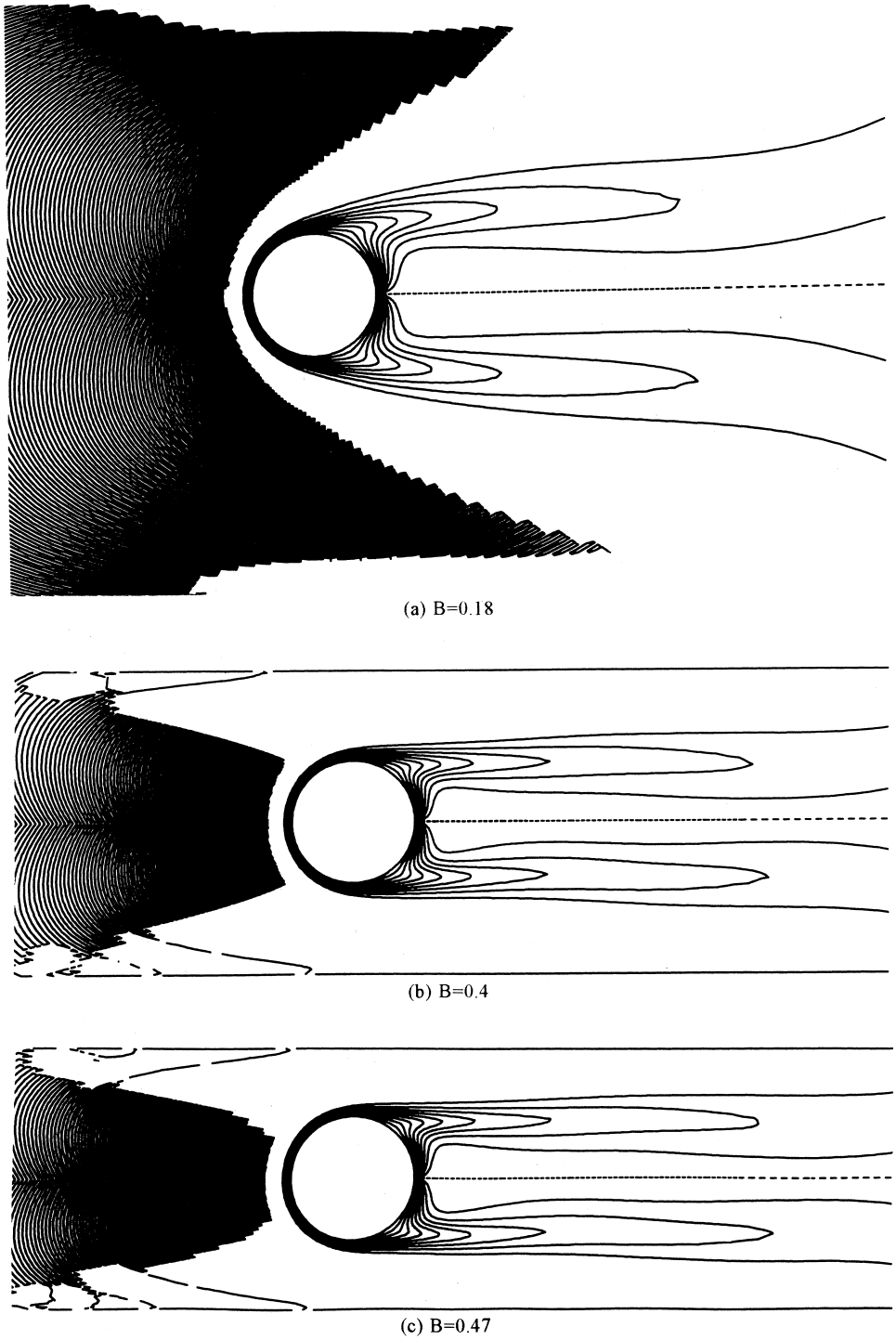

Fig. 11. Isotherms for different blockage ratios with Re = 390.

which the remaining data could be compared. A single cylinder corresponded to blockage ratio of 0.18, additional tubes were added to produce blockage ratios of 0.4 and 0.47. Upstream velocity measurements were obtained using a hot wire probe.

4. Results and discussion

For a cylinder in cross-flow a laminar boundary layer develops from the front stagnation point and grows in thickness around the cylinder. Separation of the laminar boundary layer takes place when the low velocity fluid close to tube wall can no longer overcome the adverse pressure gradient over the rear portion of the tube and the flow stalls forming a region of reverse flow close to the surface. This reverse flow is confined to the region between the separation point and the rear stagnation point and so a vortex is established on each rear half of the cylinder. Zukauskas (1972) studied how this process varies with Reynolds number. When Reynolds number is smaller than 1, inertial forces are negligible relative to the viscous forc-

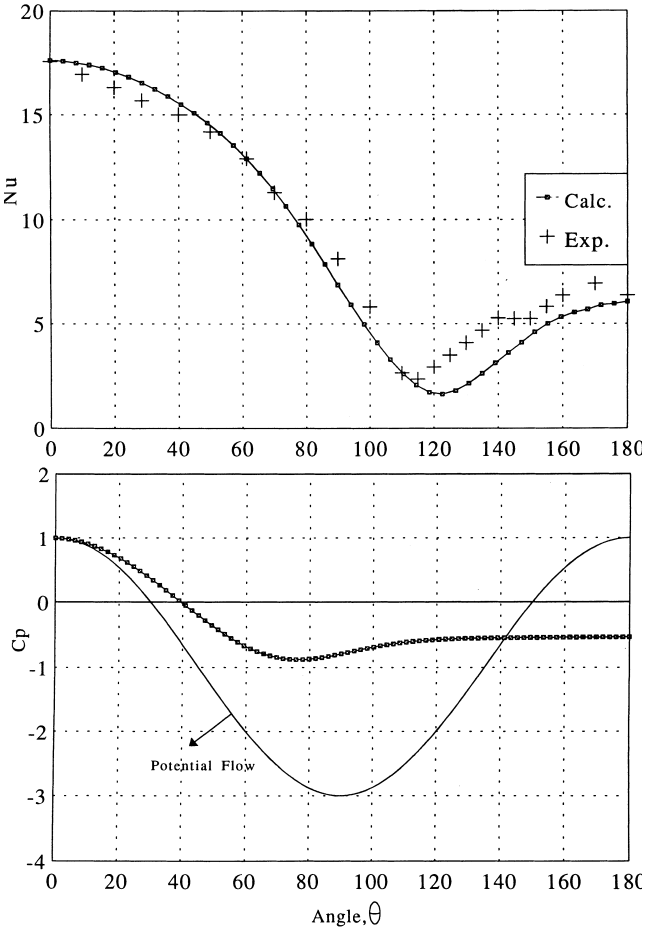

Fig. 12. Calculated and measured local Nusselt number and calculated pressure coefficient for $B = 0.18$ and $\mathrm{Re} = 390$.

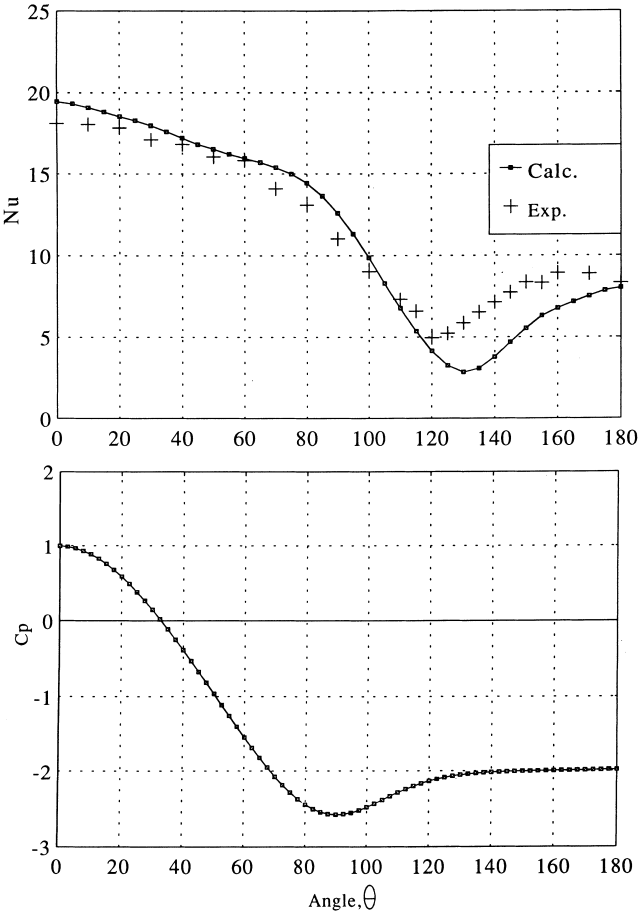

Fig. 13. Calculated and measured local Nusselt number and calculated pressure coefficient for $B = 0.4$ and $\mathrm{Re} = 390$.

es and laminar boundary layer separation takes places at the rear stagnation point. When the Reynolds number is greater than 5, the laminar boundary layer separates from the tube before the rear stagnation point, and symmetrical stable vortices are formed behind the tube. In the case of Reynolds number greater than 40 stability is lost and vortices are shed from the rear of the tube. The Reynolds number of the flow determines both the thickness of the laminar boundary layer and the point at which it separates from the tube.

Flow around circular cylinders and boundary layer separation have been investigated at various Reynolds numbers by Kraabel et al. (1982), Zukauskas (1972), Schmidt and Wenner (1943) and Boulas and Pei (1974). Variation in local Nusselt number around the cylinder is affected by the boundary layer development on the front of the tube and by separation and vortex shedding over the rear. The maximum Nusselt number occurs at the front stagnation point where the boundary layer is thinnest and hence resistance to heat transfer is at a minimum. The minimum Nusselt number is found to correspond to a point close to the boundary layer separation point. The minimum Nusselt number location is hence dependent on the Reynolds number of the flow.

In practice, circular tubes are usually in a flow channel where considerable blockage is presented and this has a great influence on the heat transfer. As blockage increases, the velocity increases outside the boundary layer and the pressure and velocity distributions change accordingly. Figs. 5–9 show the calculated laminar heat transfer and flow characteristics for a single cylinder for a Reynolds numbers of 120 and blockage ratios of 0.18–0.47. Streamline contours are shown in Fig. 5 for different blockage ratios and it is seen that the separation point moves downstream as a result of increasing blockage. It is seen from the isotherm contours in Fig. 6 that the thermal boundary layer develops around the cylinder and its thickness is very similar for the three different blockage cases prior to separation. The isotherm contours show how the thermal boundary layer thickens rapidly beyond the separation point.

In order to evaluate the accuracy of the heat transfer calculation procedure developed in this study, the local Nusselt number distribution for the low blockage case ($B = 0.18$) for a Reynolds number of 120 was compared with the data of Eckert and Soehngen (1953) for unconfined flow (experiment and calculation) as shown in Fig. 7. There is good agreement between the measurements and both calculations for most of the range. However for their calculation the minimum Nusselt number occurs later than observed at about 155°. The current calculation predicts the location of the minimum Nusselt number very well although the experimental values are slightly lower than the predicted values. This could be due to the blockage or the free convection effects which were not specified by Eckert and Soehngen. The calculated values of local Nusselt number and surface pressure for blockage ratios between 0.18 and 0.47 are shown in Figs. 7–9. The location of minimum Nusselt number and minimum pressure move downstream to the rear of the tube as the blockage is increased. The values of Nusselt number and pressure also increase with increasing blockage.

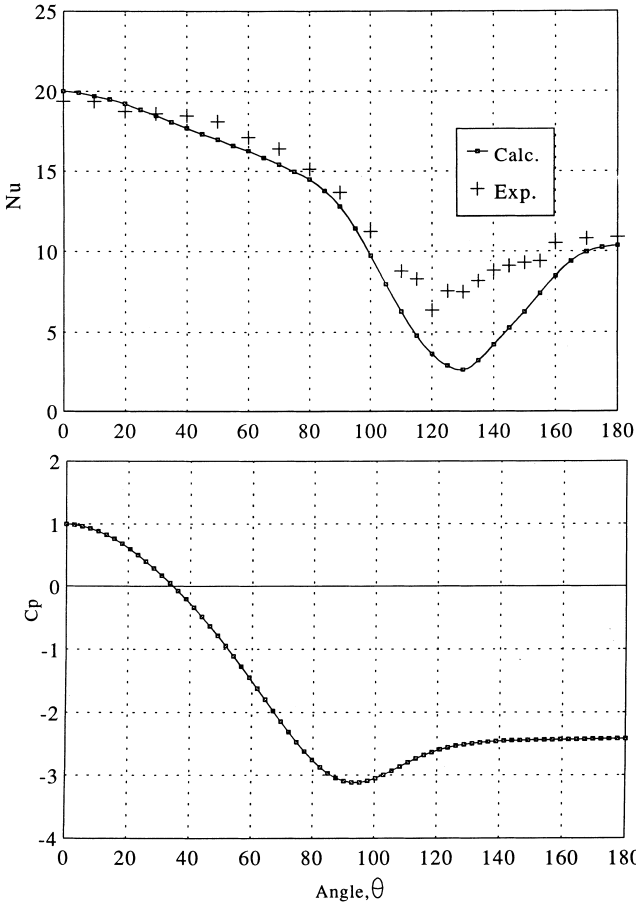

Fig. 14. Calculated and measured local Nusselt number and calculated pressure coefficient for $B = 0.47$ and $\mathrm{Re} = 390$.

Figs. 10–14 show the laminar heat transfer and flow characteristics of a single cylinder corresponding to a Reynolds number of 390 with the same blockage ratios as used for the previous case. The streamline contours can be seen in Fig. 10 which shows that the separation point moves from 115° at a blockage ratio of 0.18 further downstream by about 10° as the blockage is increased to 0.47. The effect of increasing Reynolds number is to move the separation point upstream. The isotherm contours are shown in Fig. 11 and show that the thickness of the thermal boundary layer is less than for the previous Reynolds number of 120.

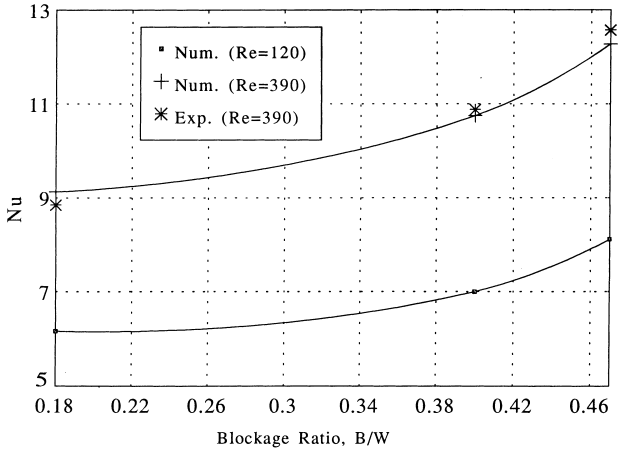

Fig. 15. Comparison of averaged Nusselt number with varying blockage ratio.

A comparison of the calculated local Nusselt number distributions and the experimental results is made in Figs. 12–14. In each case, the agreement is good up to the position at which the minimum Nusselt number is observed, close to the point at which the boundary layer separates. The numerical model predicts the separation to occur about 10° beyond that found by experiment and as a result beyond separation the predicted Nusselt numbers are lower than measured. The differences are possibly due to the fact that in the experiments the unsteady vortex shedding process will carry cool air into the wake region thereby increasing the effective temperature difference and hence the heat transfer from the surface. It can also be seen from these figures that if the separation point had been predicted accurately, the agreement beyond it would have probably been reasonably good. The failure to accurately predict the separation point is also related to the fact that there will not be a fixed, steady separation point and wake, but a periodic one. This unsteady effect is not modelled in the numerical calculations which use the time averaged Navier–Stokes equations.

Considering the overall heat transfer from the cylinder, this can be found by integrating the heat transfer coefficient to calculate the average Nusselt number as shown in Fig. 15. Again the satisfactory agreement between experiment and prediction can be seen.

5. Conclusions

Numerical calculations have been carried out for laminar flow and heat transfer for flow past a single cylinder in a row of cylinders. The numerical investigation has considered the effect of blockage and Reynolds number on the heat transfer and flow characteristics. Calculations have been carried out for Reynolds numbers of 120 and 390 and blockage ratios between 0.18 and 0.47. The results were compared with experiment. The main conclusions are as follows:

- Increased blockage causes the separation point to move downstream. Experimental separation point locations did not always agree well with the flow predictions.
- Increasing blockage increased the heat transfer rate from the cylinder.
- Increasing Reynolds number causes the point of separation to move upstream and the overall heat transfer to increase.
- The agreement between measured and numerically predicted heat transfer distributions was generally satisfactory except for the rear of the cylinder because of the difficulty of predicting accurately the separation point. Unsteady time dependent calculations are needed to model the periodic vortex shedding process.

References

Antonopolous, K.A., 1985. Heat transfer in tube assemblies under conditions of laminar axial, transverse and inclined flow. Int. J. Heat & Fluid Flow 6 (3), 193–204.

Bergelin, O.P., Davis, E.S., Hull, H.L., 1949. A study of three tube arrangements in unbaffled tubular heat exchangers. Trans. ASME 71, 369–374.

Boulas, M.J., Pei, D.C.T., 1974. Dynamics of heat transfer from cylinders in a turbulent airstream. Int. J. Heat and Mass Transfer 17, 767–783.

Buyruk, E., Barrow, H., Owen, I. 1995. The influence of adjacent tubes on Convection Heat Transfer from a Heated Tube in Cross-flow.

In: Fourth UK National Conference on Heat Transfer, I. Mech. E. Conference Trans., pp. 135–139.

Chen, C.K., Wong, K.I., Cleaver, J.W., 1986. Finite element solutions of laminar flow and heat transfer of air in a staggered and an in-line tube bank. Int. J. Heat & Fluid Flow 7 (4), 291–300.

Dennis, S.C.R., Hudson, J.D., Smith, N., 1968. Steady laminar forced convection from a circular cylinder at low Reynolds numbers. The Physics of Fluids 11 (5), 933–940.

Eckert, E.R.G., Soehngen, E. 1953. Distribution of heat transfer coefficients around circular cylinders in cross-flow at Reynolds number from 20 to 500. Trans. ASME, Paper 51-F9, pp. 343–347.

Faghri, M., Rao, N., 1987. Numerical computation of flow and heat transfer in finned and unfinned tube banks. Int. J. Heat mass transfer 30 (2), 363–372.

Hiwada, M., Mabuchi, U., 1980. Flow behaviour and heat transfer around a circular cylinder at high blockage ratios. Trans. JSME 46 (409), 52–61.

Johnson, M.W., 1990. Computation of flow in a vortex-shedding flowmeter. Flow Meas. Instrum. 1, 201–208.

Kraabel, J.S., McKillop, A.A., Baughn, J.W., 1982. Heat Transfer to Air form a Yawed Cylinder. Int. J. Heat and Mass Transfer 25, 409–418.

Krall, K.M., Eckert, E.R.G., 1973. Local heat transfer around a cylinder at low Reynolds number. Trans. ASME: J. Heat Transfer 95, 273–275.

Kreith, F., 1965. Principles of Heat Transfer, 2nd Edition. Int. Textbook Company, London.

Launder, B.E., Massey, T.H., 1978. The numerical prediction of viscous flow and heat transfer in tube bank. Trans. ASME: J. Heat Transfer 100, 565–571.

Omohundro, C.A., Bergelin, O.P., Colburn, A.P., 1949. Heat transfer and fluid friction during viscous flow across banks of tubes. Trans. ASME 71, 27–34.

Paolino, M.A., Kinney, R.B., Cerutti, E.A., 1986. Numerical analysis of the unsteady flow and heat transfer to a cylinder in crossflow. Trans. ASME: J. Heat Transfer 108, 742–748.

Perkins, H.C., Leppert, G., 1964. Local heat transfer coefficients on a uniformly heated cylinder. Int. J. Heat and Mass Transfer 7, 143–158.

Schmidt, E., Wenner, K., 1943. Heat transfer over the circumference of a heated cylinder in transverse flow. NACA Technical Memorandum, p. 1050.

Thompson, J.F., Thomes, F.C., Mastin, C.W., 1974. Automatic numerical generation of body fitted curvilinear coordinate system for field containing any number of arbitrary two dimensional bodies. J. Comput. Phys. 15, 299–319.

West, G.S., Apelt, C.J., 1982. The effect of tunnel blockage and aspect ratio on the mean flow past a circular cylinder with Reynolds number between 10^4 and 10^5. J. Fluid Mech. 114, 361–377.

Zdravistch, F., Clive, A.F., Behnia, M., 1995. Numerical laminar and turbulent fluid flow and heat transfer predictions in tube banks. Int. J. Num. Meth. Heat Fluid Flow 5, 717–733.

Zukauskas, A., 1972. Heat transfer from tubes in cross-flow. Advances in Heat Transfer 8, 93–160.